BB

BCCNT 95/032/245

Chiral Symmetry in Nuclear Physics:

A Physical Interpretation of Correlated Two-Pion Exchange

L.S. Celenza, C.M. Shakin, Wei-Dong Sun, and J. Szweda

Department of Physics and Center for Nuclear Theory

Brooklyn College of the City University of New York

Brooklyn, New York 11210

(March, 1995)

Submitted to Physical Review C (Subnucleon Aspects of Nuclei/Physics of Hadrons)

Abstract

We use a coupled-channel quark-hadron model to provide a description of correlated two-pion exchange. We consider the amplitudes for $N + \bar{N} \to \pi + \pi$ and $q + \bar{q} \to \pi + \pi$ for positive t-channel energy, where two-pion production is a physical process. As is well known, when the Mandelstam variable t becomes spacelike, one can replace the two-pion exchange process by the exchange of an effective low-mass scalar-isoscalar (sigma) meson. In the context of our coupled-channel model, we show that that sigma meson is the chiral partner of the pion. This identification proceeds via the bosonization of a generalized Nambu−Jona-Lasinio (NJL) model which provides the basis for our coupled-channel model. In our analysis, we find that the linear sigma model, that may be obtained by bosonization of the NJL model, is useful if the meson momenta are spacelike. (That is the case in studies of nuclear structure and nucleon-nucleon scattering made using boson-exchange models.) Although some aspects of our work are qualitative, we believe our analysis provides an advance in our understanding of the physical significance of correlated two-pion exchange and relates that description of the origin of the intermediate-range nucleon-nucleon interaction to chiral symmetry.

I. Introduction

The origin of the scalar attraction in the intermediate-range nucleon-nucleon interaction has been of interest for some time. For example, in the one-boson-exchange model of the nucleon-nucleon interaction that potential arises from the exchange of a sigma meson of mass $m_\sigma \simeq 550$ MeV [1]. Since there is no such meson in the data tables, sigma exchange is thought to approximate other effects. In a rather elegant body of work [2-5], that made use of dispersion relations and our knowledge of the amplitude $N + \bar{N} \rightarrow \pi + \pi$ (taken from the study of $\pi - N$ scattering), it was seen that the exchange of the sigma could be understood as representing "correlated two-pion exchange". (We will define that term in the following discussion.) When obtaining an understanding of the origin of an (effective) sigma meson in this manner, one does not have an understanding of the role of chiral symmetry in the nucleon-nucleon force. For example, we may ask if the chiral partner of the pion plays an important role in the nucleon-nucleon force. We may also ask for the relation of the (effective) sigma that substitutes for correlated two-pion exchange and the chiral partner of the pion. This entire issue is made more confusing by the fact that there is no physical low-mass sigma meson and, therefore, the nonlinear sigma model is the model most extensively used in elementary particle physics [6].

One may also note that the Nambu–Jona-Lasinio (NJL) model [7] yields a low-mass sigma meson ($m_\sigma \simeq 2m_q$) upon bosonization [8]. In earlier work we have shown how to extend the model to include confinement and how to take into account the coupling of the sigma to the two-pion continuum. We have also shown how those features can eliminate the sigma as a low-mass physical particle. However, we found that if the sigma momentum is spacelike, the

sigma is a useful degree of freedom [9,10]. (We note that, for spacelike momentum, the sigma is largely uncoupled from the two-pion continuum.)

In this work our goal is to use our coupled-channel quark-hadron model to understand the nature of correlated two-pion exchange and to make the connection to chiral symmetry. Our result will identify the (effective) sigma that simulates correlated two-pion exchange with the chiral partner of the pion. In this fashion we obtain a unified point of view relating Dirac phenomenology [11], QCD sum rules in matter [12] and the boson-exchange model of the nucleon-nucleon force [1]. As we will see, our work clarifies the role of chiral symmetry in various aspects of nuclear structure physics.

II. Correlated Two-Pion Exchange in Pion-Nucleon Scattering

In order to define correlated two-pion exchange and fix the notation, we will closely follow the recent work of Schütz, Durso, Holinde, and Speth [13]. The variables are as shown in Fig. 1. The T matrix is defined in terms of the S matrix:

$$S_{fi} = \delta_{fi} - i(2\pi)^4 \delta^{(4)}(P_f - P_i) \left[\frac{1}{(2\pi)^{3/2}}\right]^4 \left[\frac{m_N}{E_p}\frac{m_N}{E_{p'}}\right]^{1/2} (2\omega_q \cdot 2\omega_{q'})^{-1/2} T_{fi} \quad . \tag{2.1}$$

Here $E_p = (p^2 + m_N^2)^{1/2}$ and $\omega_q = (q^2 + m_\pi^2)^{1/2}$, etc. Then, for the s-channel process, $\pi + N \to \pi + N$, the T matrix is written as

$$T_s(p', q'; p, q) = \bar{u}(p', \lambda')\, \xi^\dagger(\mu')\zeta^\dagger(\beta)\, \hat{T}(s,t)\, u(p, \lambda)\xi(\mu)\zeta(\alpha) \quad , \tag{2.2}$$

where λ is a helicity index, while ξ and ζ are isospin wave functions of the nucleon and pion, respectively. One then writes

$$\hat{T}(s,t) = \hat{T}^{(+)}(s,t) - \hat{T}^{(-)}(s,t)\tau \cdot t \quad , \tag{2.3}$$

where τ and t are the isospin matrices for the nucleon and pion, respectively. With $Q = \frac{1}{2}(q + q')$, we have

$$\hat{T}^{(\pm)}(s,t) = -\left[A^{(\pm)}(s,t) + \not{Q}B^{(\pm)}(s,t)\right] \quad . \tag{2.4}$$

In the t channel ($N\bar{N} \to 2\pi$) the amplitude T is

$$T_t(q', \bar{q}'; \bar{p}, p) = \bar{v}(\bar{p}, \lambda')\bar{\xi}^{\dagger}(\mu')\zeta^{\dagger}(\beta)\hat{T}(s,t)u(p,\lambda)\xi(\mu)\zeta(\alpha) \quad , \tag{2.5}$$

with $\bar{p} = -p'$ and $\bar{q}' = -q$. Here $\bar{v}$ is the Dirac spinor of an antinucleon, etc. [13].

The next step is to perform a partial-wave decomposition for $A^{(\pm)}$ in the t channel,

$$A^{(\pm)}(s,t) = \sum \frac{1}{2}(2J+1)P_J(x)A_J^{(\pm)}(t) \quad , \tag{2.6}$$

with the same expression for $B^{(\pm)}$. Here $P_J(x)$ is a Legendre function of $x = \cos\theta_t$, where θ_t is the scattering angle in the t channel, which may be expressed in terms of s and t [13]. One defines

$$f_+^J(t) = \frac{1}{8\pi}\left[\frac{-p_t^2}{(p_t q_t)}A_J^{(+)} + \frac{m_N}{(2J+1)(p_t q_t)^{J-1}}\left[(J+1)B_{J+1}^{(+)} + JB_{J-1}^{(+)}\right]\right] \tag{2.7}$$

and also an amplitude $f_-^J(t)$. Here $p_t = |p|$ and $q_t = |q|$ are defined in the c.m. system for the t-channel process.

If we limit ourselves to consideration of $f_+^0(t)$, we have

$$f_+^0(t) = \frac{1}{8\pi}(-p_t^2)A_0^{(+)}(t) \quad . \tag{2.8}$$

Note that $f_-^{J=0}(t) = 0$ and that, in general, $p_t^2 = t/4 - m_N^2$.

One can write a dispersion relation for $f_+^0(t)/(t/4 - m_N^2)$ and make use of the knowledge of $\mathrm{Im} f_+^0(t)$. [See Fig. 2.] With $a = 4m_\pi^2(1 - m_\pi^2/4m_N^2)$, we have

$$\frac{f_t^0(t)}{t/4 - m_N^2} = \frac{1}{\pi}\int_{-\infty}^{a} dt' \; \frac{1}{t' - t - i\epsilon} \frac{\mathrm{Im} f_+^0(t')}{\left(\frac{t'}{4} - m_N^2\right)} + \frac{1}{\pi}\int_{4m_\pi^2}^{\infty} dt' \; \frac{1}{t' - t - i\epsilon} \frac{\mathrm{Im} f_+^0(t')}{\left(\frac{t'}{4} - m_N^2\right)} \quad . \tag{2.9}$$

The second term in Eq. (2.9) represents the contribution of correlated two-pion-exchange [13]. For that contribution alone, one defines $\tilde{f}_+^0(t)$ and an amplitude

$$A_\sigma^{(+)}(t) = -\frac{4\pi}{p_t^2}\tilde{f}_+^0(t) \quad , \tag{2.10}$$

$$= -16\int_{4m_\pi^2}^{\infty} dt' \; \frac{\mathrm{Im} f_+^0(t')}{(t' - t)(t' - 4m_N^2)} \quad . \tag{2.11}$$

(See Eq. (30) of Ref. [13].)

We anticipate that $A_\sigma^{(+)}(t)$ can be written as

$$A_\sigma^{(+)}(t) \simeq -\frac{2g_{\sigma\pi\pi}G_{\sigma NN}}{t - m_\sigma^2} \tag{2.12}$$

with $g_{\sigma\pi\pi}$ and $G_{\sigma NN}$ of the same sign. (That sign choice follows from the structure of Eq. (2.9), for example.) We may use a value for the sigma-nucleon coupling constant, $G_{\sigma NN}$, obtained from the one boson-exchange model of the nucleon-nucleon interaction. The value

given in Ref. [1] is about 9 or 10 for $G_{\sigma NN}$, if no explicit reference is made to the delta (1232 MeV) resonance. The value of $g_{\sigma\pi\pi}$ may be obtained from the linear sigma model, if the sigma is to be identified with the chiral partner of the pion. (We will return to this point shortly.)

We note that the authors of Ref. [13] perform a subtraction so that the subtracted amplitude, $A_\sigma^{(+)'}(t)$, is zero at the Cheng-Dashen point [14]. If Eq. (2.10) is a correct representation, we would define

$$A_\sigma^{(+)'}(t) = A_\sigma^{(+)}(t) - A_\sigma^{(+)}(2m_\pi^2) \quad , \tag{2.13}$$

$$= \frac{2g_{\sigma\pi\pi}G_{\sigma NN}}{m_\sigma^2 - 2m_\pi^2} \frac{t - 2m_\pi^2}{m_\sigma^2 - t} \quad , \tag{2.14}$$

which has the structure of Eq. (38) of Ref. [13]. We will not be concerned with the subtracted form, since that can easily be obtained.

Returning to Eqs. (2.11) and (2.12), we see that we can obtain a measure of the product $g_{\sigma\pi\pi}G_{\sigma NN}$ by comparing Eq. (2.11) and Eq. (2.12) for large $-t$. We have

$$g_{\sigma\pi\pi}G_{\sigma NN} \simeq -8 \int_{4m_\pi^2}^{t_c} dt' \frac{\mathrm{Im}\, f_+^0(t')}{(t' - 4m_N^2)} \quad , \tag{2.15}$$

where t_c is the maximum value of t considered ($t_c \sim 1$ GeV^2). If we use $G_{\sigma NN} \sim 3g_{\sigma qq} \sim 9$ and $g_{\sigma\pi\pi} = m_\sigma^2/2f_\pi$, with $m_\sigma = 0.50$ GeV, we find that Eq. (2.15) is well satisfied indicating that Fig. 1(b) provides a satisfactory model for the process $N + \bar{N} \to \pi + \pi$. Here, the use of $g_{\sigma\pi\pi} = m_\sigma^2/2f_\pi$ identifies the sigma meson as the chiral partner of the pion. This identification

will be made more precise in the next section, where we study the amplitude for a quark and an antiquark to go to two pions ($q + \bar{q} \to \pi + \pi$).

III. Coupled-Channel Quark-Hadron Models

We have developed coupled equations describing the scattering of a quark and antiquark, with the coupling to the two-pion continuum included in the model [9,10]. For this purpose we make use of the NJL model, generalized to include a description of confinement [15]. One form of the coupled equations is shown in Fig. 3. There we define T matrices, t_{qq}, $t_{\pi\pi}$, and $t_{q\pi}$. The first of these T matrices describes quark-antiquark scattering, the second describes pion-pion scattering and the last is the amplitude to go from the $q\bar{q}$ channel to the two-pion channel. In our work we did not aim to provide a good fit to elastic $\pi - \pi$ scattering, nor did we attempt to impose crossing symmetry on the amplitudes. We were mainly concerned with demonstrating how the coupled-channel aspects of the problem affect the simple results obtained in the bosonization of the NJL model at one-loop order [8]. (We do not solve the coupled equations in their most general form, but limit ourselves to approximations that allow us to express the T matrices in terms of two basic loop integrals.)

Some of our results are best understood by inspection of a series of diagrams. In Fig. 4(a) we show the basic quark-loop integral of the NJL model, for $t = P^2$,

$$-iJ_S(P^2) = (-1)n_c n_f \int d^4k \; iS(P/2 + k) \; iS(-P/2 + k) \quad , \tag{3.1}$$

where $n_c = 3$ and $n_f = 2$ are the number of colors and flavors, respectively. Further, the quark propagator is $S(p) = (\not{p} - m_q + i\epsilon)^{-1}$, with m_q being the constituent quark mass. As we

have discussed in earlier work, it is possible to generalize the analysis to include a model of confinement through the introduction of a linear potential V^C. Upon summing a ladder of interactions, the confining potential gives rise to a vertex shown as a cross-hatched area in Fig. 4(b). That vertex has the property of vanishing when both the quark and antiquark go on mass shell [15]. If that vertex is included, we replace $J_S(P^2)$ by $\hat{J}_S(P^2)$, where $\hat{J}_S(P^2)$ is a <u>real</u> function. That function is real, since our model of confinement serves to remove the $q\bar{q}$ cuts that are unphysical aspects of the NJL model. Because of that feature, we are able to write dispersion relations for various amplitudes. The dispersion relations involve discontinuities across only <u>physical</u> cuts that correspond to hadrons going on mass shell [16,17]. The important cut in our analysis appears for $t \geq 4m_\pi^2$.

In Fig. 4(c) we define the function $K_S(P^2)$. There, the wavy lines are pions and $K_S(P^2)$ has an imaginary part corresponding to the two pions going on mass shell. Cuts that would arise when the quark and antiquark go on mass shell are eliminated in the function $\hat{K}_S(P^2)$ of Fig. 4(d) by including the vertex function of the confining potential. It is also useful to define the function $\hat{M}(P^2) = -G_S^2\hat{K}_S(P^2)$. Values for the real and imaginary parts of $\hat{M}(P^2)$ are given in Fig. 5, which is taken from Ref. [9]. (Recall that $t = P^2$ in this analysis.)

We have considered various approximations in the solution of the coupled equations. We will refer to two of these models: model B[9] and model C[16]. Both of these models neglect the box diagrams that have the structure indicated in Fig. 6(a). Model B differs from model C in that we also neglect the diagram shown in Fig. 6(b) in model B.

The T matrix of model C is particularly simple in the scalar-isoscalar channel of the quark and antiquark,

$$t_{qq}^{C}(t) = -\frac{G_S}{1 - G_S[\hat{J}_S(t) + \hat{K}_S(t)]} \quad . \tag{3.2}$$

(We have now replaced P^2 by t in accordance with the notation of Sec. II.) The T matrix of model B is [9]

$$t_{qq}^{B}(t) = -\frac{G_S[1 + G_S\hat{K}_S(t)]}{1 - G_S[1 + G_S\hat{K}_S(t)]\hat{J}_S(t)} \quad . \tag{3.3}$$

The various diagrams summed by this T matrix are shown in Fig. 6(c). (Note the absence of adjoining factors of $\hat{K}_S(t)$.) The T matrices of Eqs. (3.2) and (3.3) do not represent the most general T matrices one can construct. They are T matrices that may be expressed in terms of $\hat{J}_S(t)$ and $\hat{K}_S(t)$ only.

It is also useful to define

$$D^{C}(t) = 1 - G_S\hat{J}_S(t) - G_S\hat{K}_S(t) \quad , \tag{3.4}$$

and

$$D^{B}(t) = 1 - G_S\hat{J}_S(t) - G_S^2\hat{K}_S(t)\hat{J}_S(t) \quad , \tag{3.5}$$

which are the denominators of Eqs. (3.2) and (3.3), respectively.

We recall that Im $\hat{K}_S(t)$ is nonzero for $t \geq 4m_\pi^2$. It is very important to see that the approximation of neglecting the third term on the right-hand side of Eq. (3.4) or Eq. (3.5) is good for $t < 0$. For example, at $t = 0$ we find $D^{B}(0) = 1 - 0.63 - 0.044$, so that we see that the last term is only a rather small correction. As t becomes increasingly negative, the third

term becomes even smaller. [See Fig. 5.] Therefore, for $t < 0$ we will drop $\hat{K}_S(t)$, with the result that for both of the T matrices given above, we have

$$t_{qq}(t) = -\frac{G_S}{1 - G_S \hat{J}_S(t)} \quad , \tag{3.6}$$

$$= \frac{g^2_{\sigma qq}(t)}{t - m^2_\sigma(t)} \quad , \tag{3.7}$$

$$\simeq \frac{g^2_{\sigma qq}}{t - m^2_\sigma} \quad , \tag{3.8}$$

where $g_{\sigma qq} = g_{\sigma qq}(0)$ and $m_\sigma = m_\sigma(0)$. Equation (3.7) is an exact result of the momentum-space bosonization scheme of Bernard, Osipov, and Meissner [8], while Eq. (3.8) is an approximation valid if t does not go over a large range. (These forms are to be used for spacelike t, as specified above.)

To make contact with the work of the last section, we consider the amplitude $q + \bar{q} \to \pi + \pi$ in the scalar-isoscalar channel. The formalism describing the amplitude $N\bar{N} \to \pi + \pi$ in the last section may be used with m_N replaced by m_q. However, because of the model of confinement we have introduced, we may drop the factor $(t/4 - m_q^2)$ that could be used to relate $f^0_+(t)$ to $A^{(+)}_0(t)$, since there are no cuts associated with the quark and the antiquark going on mass shell.

Now consider the $q + \bar{q} \to \pi + \pi$ amplitude shown in Fig. 7(a). In Fig. 7(b) we indicate the diagrammatic expansion of that amplitude. We write

$$t^B_{q\pi}(t) = t^B_{qq}(t)F(t) \quad , \tag{3.9}$$

where *F(t)* denotes the diagrammatic element shown in Fig. 7(c).

For $t < 0$ we can neglect $\hat{K}_S(t)$ to a good approximation. We then have the series of Fig. 8(a). An approximation to the process shown in Fig. 8(a) is shown in Fig. 8(b). Again, if $\hat{K}_S(t) \simeq 0$, we have from Eq. (3.9)

$$t^B_{q\pi}(t) \simeq -\frac{G_S F(t)}{1 - G_S \hat{J}_S(t)} \quad , \tag{3.10}$$

$$\simeq \frac{g^2_{\sigma qq} F(t)}{t - m^2_\sigma} \quad . \tag{3.11}$$

Therefore, we can see that

$$g_{\sigma qq} F(t) \simeq 2 g_{\sigma\pi\pi} \tag{3.12}$$

for small t. Here, $g_{\sigma\pi\pi}$ may be obtained from direct evaluation of *F(t)*, or from the linear sigma model, where

$$g_{\sigma\pi\pi} \simeq \frac{m^2_\sigma}{2 f_\pi} \quad , \tag{3.13}$$

if the $\sigma\pi\pi$ coupling of the linear sigma model is written as

$$\mathcal{L}_I(x) = - g_{\sigma\pi\pi} \sigma(x) \pi(x) \cdot \pi(x) \quad . \tag{3.14}$$

Now let us make contact with the formalism of correlated two-pion exchange. We have considered correlated two-pion exchange in detail in a calculation of the scalar-isoscalar correlation function,

$$iC(P^2) = \int d^4x e^{iP\cdot x}\langle 0|T(\bar{q}(x)q(x)\bar{q}(0)q(0))|0\rangle \tag{3.15}$$

in Ref. [9]. In the calculation of Im $C(P^2)$ we took into account only the right-hand cut starting at $P^2 = t = 4m_\pi^2$. We then obtained Re $C(P^2)$ via a dispersion relation,

$$C(P^2) = -\hat{J}_S(P^2) - \frac{1}{\pi}\int_{4m_\pi^2}^{\infty} \frac{\text{Im } C(P'^2)}{P^2 - P'^2 + i\epsilon} \quad . \tag{3.16}$$

In practice, the upper limit for the integral is about $P^2 = 1$ GeV^2. [See Fig. 9.] We should note that in Ref. [9] we wrote the dispersion relation of Eq. (3.16) without including $\hat{J}_S(P^2)$. Therefore, Re $C(P^2)$ obtained there via the dispersion relation should be properly defined to be Re $C(P^2) + \hat{J}_S(P^2)$. (See Fig. 9, where the caption has been corrected relative to the corresponding figure in Ref. [9].)

The relation of $t_{qq}(t)$ to $C(t)$ was discussed in a previous work [16]. However, the $C(t)$ given in Ref. [16] was defined as the negative of the $C(t)$ used here and in Ref. [9]. For the sign convention of the current work, we have for $t < 0$, where we can neglect $\hat{K}_S$ in a first approximation,

$$C(t) = -\hat{J}_S(t) + \hat{J}_S(t)t_{qq}(t)\hat{J}_S(t) \quad , \tag{3.17}$$

or

$$t_{qq}(t) = \frac{C(t) + \hat{J}_S(t)}{[\hat{J}_S(t)]^2} \quad . \tag{3.18}$$

The approximation relations given in Eqs. (3.17) and (3.18) should not be used for $t > 0$, or where an accurate calculation is desired.

Again considering the region $t < 0$, we saw that $t_{qq}(t)$ and $C(t)$ were very well approximated in a sigma-dominance model [9]. We have, if Re $\hat{K}_S(t) = 0$,

$$C(t) + \hat{J}_S(t) = \frac{\hat{J}_S^2(t) g_{\sigma qq}^2}{t - m_\sigma^2} \qquad t < 0 \quad , \tag{3.19}$$

(see Fig. 9) and we also have

$$t_{qq}(t) = \frac{g_{\sigma qq}^2}{t - m_\sigma^2} \tag{3.20}$$

to a good approximation. Thus, from Eq. (3.9) we see that, for $t < 0$,

$$t_{q\pi}(t) = \frac{g_{\sigma qq}^2}{t - m_\sigma^2} F(t) \quad . \tag{3.21}$$

We may also define an amplitude

$$\tilde{f}_q^0(t) = -\frac{m_q^2}{4\pi} t_{q\pi}^B(t) \quad , \tag{3.22}$$

so that, for $t < 0$,

$$\tilde{f}_q^0(t) = -\frac{m_q^2}{4\pi}\frac{g_{\sigma qq}^2}{t-m_\sigma^2}F(t) \quad . \tag{3.23}$$

This amplitude is the analog of the amplitude $\tilde{f}_+^0(t)$ considered in Sec. II. (See Eq. (2.10).)

At this point we have reached our goal of demonstrating that the dynamics of correlated two-pion exchange can be represented (for $t < 0$) by a sigma dominance model, where the sigma is the chiral partner of the pion. That identification appears in the passage from Eq. (3.10) to Eq. (3.11), where we use the basic relation for the bosonization of the NJL model at one-loop order [8].

IV. Calculation of $\hat{J}_S(t)$ and $F(t)$.

We are interested in values of $\hat{J}_S(t)$ and $F(t)$ in both the spacelike and timelike regions of t. For $t < 0$, the inclusion of confinement leads to only a small difference between $J_S(t)$ and $\hat{J}_S(t)$. Therefore, in the spacelike domain we can neglect confinement and calculate $J_S(t)$ and $F(t)$ by going over to a Euclidean momentum space and making use of the Feynman parametrization of the integrals. For $t > 0$, however, we work in Minkowski space and incorporate the vertex functions of the confining field, V^C [15].

Results obtained in this manner are shown in Figs. 10 and 11. In Fig. 10 we see a small difference between $J_S(t)$ and $\hat{J}_S(t)$ at $t = 0$. That reflects the fact that $\hat{J}_S(0)$, which is calculated with the inclusion of the vertex functions of the confining potential, is slightly smaller than $J_S(0)$ calculated without the vertex function. The dashed curve gives the values of $J_S(t)$ for $t > 0$. (Use of that curve for $t > 0$ would lead to a physical sigma meson of mass $m_\sigma = (4m_q^2 + m_\pi^2)^{1/2} = 542$ MeV [8].) We note that for the calculation for $t < 0$, we used

a Euclidean momentum space cutoff of $\Lambda = 1.0$ GeV, while in Minkowski space we used a cutoff on all three-momenta appearing in our integrals of $\Lambda_3 = 0.702$ GeV. (This difference in the values of the cutoffs used in the two types of calculation is typical of other work in this field.)

In Fig. 11 we exhibit values calculated for $F(t)$. The solid line for $t < 4m_\pi^2$ is calculated in Euclidean momentum space neglecting confinement, while for $t > 4m_\pi^2$ we include the effects of confinement.

Before going on to a discussion of the nucleon-nucleon interaction, in Fig. 12 we illustrate the sigma-dominance results obtained for the quark-quark scattering amplitude t_{qq}, the pion production amplitude, $t_{q\pi}$, and the correlation function $C(t) + \hat{J}_S(t)$. These various representations are valid for $t < 0$. For completeness, we present values of $t_{qq}(t)$ and $t_{q\pi}(t)$ in Figs. 13 and 14, respectively. There we make use of model B. [See Eq. 3.3).]

Inspection of Fig. 10 indicates that model B and C would have a scalar-isoscalar resonance with $m \sim 850$ MeV for $G_S = 7.91$ GeV^{-2}. While there is a scalar-isoscalar resonance, the $f_0(975)$, in the data tables, it is thought that resonance may not be of $q\bar{q}$ structure. (It has been suggested that the state at 975 MeV may be a multiquark state or a state with $K\bar{K}$ structure.) Therefore, in Ref. [9] we used a G_S that was reduced somewhat for the larger values of P^2. That had the effect of moving the scalar-isoscalar resonance of the model to energies higher than 1 GeV. Therefore, that resonance does not appear in the figures representing $C(t)$, $t_{qq}(t)$, $t_{q\pi}(t)$, etc.

V. The Nucleon-Nucleon Interaction

Recently there have been a number of attempts to describe the nucleon-nucleon interaction making use of various ideas concerning chiral symmetry [20-23]. However, it has been pointed out that the advantages of using the boson-exchange model are such that one might suspect that the implementation of chiral symmetry is not all that important for the description of the nucleon-nucleon interaction [24].

In this work we take a somewhat intermediate position, stressing that chiral symmetry is extremely important at the level of quarks. After bosonization of a model such as the NJL model, one finds the various mesons that play an important role in the boson-exchange model. The problem is then to specify how these mesons are coupled to the nucleon. In this program the interpretation of correlated two-pion exchange is particularly important. For example, it is necessary to counter the argument that the intermediate-range nucleon-nucleon attraction is due correlated two-pion exchange and that the relation to chiral symmetry of such dynamics is either absent or obscure [24]. Our point of view is that the boson-exchange model is satisfactory and that the challenge is to relate that model to an underlying quark model that exhibits chiral symmetry. For example, on the left-hand side of Fig. 15 we show the generic diagram used in the discussions of correlated two-pion exchange. From our point of view that process is best evaluated as in Fig. 15. In the second figure in (a) the black filled circle denotes the quark-quark interaction of the NJL model. The third diagram of (a) introduces the quark-quark correlation function $C(t)$. In Fig. 15(b) the correlation function is expressed in terms of $\hat{J}_S(t)$ and a general quark-quark T matrix. In this work, rather than using a general form for the T matrix, we use either $t^B_{qq}(t)$ or $t^C_{qq}(t)$. For $t > 4m_\pi^2$, these T matrices exhibit a two-pion

cut and describe correlated two-pion exchange. However, as we go to $t < 0$, we may use $t_{qq}(t) = -G_S/[1 - G_S\hat{J}_S(t)]$ for either model, as discussed above. That leads immediately to Fig. 15(c). The implication is that we may obtain a unified approach to correlated two-pion exchange and to a boson-exchange picture based upon chiral symmetry at the quark level.

VI. Discussion

We have seen that correlated two-pion exchange may be represented by the exchange of a "sigma meson", if t is less than zero. However, our analysis shows that that low-mass scalar-isoscalar meson is the chiral partner of the pion. That is most readily seen in the bosonization of the NJL model [8], where the relation

$$-\frac{G_S}{1 - G_S\hat{J}_S(t)} = \frac{g^2_{\sigma qq}(t)}{t - m^2_\sigma(t)} \tag{6.1}$$

is valid. The amplitude $q + \bar{q} \to \pi + \pi$ in the region of spacelike t, where Re $\hat{K}_S(t)$ may be neglected, is then given by the diagrams of Fig. 6. On the other hand, in the region where t is timelike ($t > 0$) our model essentially reproduces the structures expected from the consideration of correlated two-pion exchange. Our ability to span both the timelike and spacelike values of t depends upon having a coupled-channel quark-hadron model of the type developed in Refs. [9] and [10]. (In this discussion, it is important to keep in mind that the sigma meson does not appear as a physical particle in our model.)

Recently, we have seen a number of works that use a microscopic model of correlated two-pion exchange to study nucleon-nucleon scattering [26] and pion-nucleon scattering [27]. These models make use of a meson-exchange model of pion-pion scattering introduced earlier

[28]. In Ref. [28], pion-pion scattering in the $J = 0^+$, $T = 0$ channel is mainly governed by t-channel rho exchange and effects of the coupling to the $K\bar{K}$-channel. There is also a quite small effect due to the $f_0(1400)$ which appears as a distant s-channel resonance. (These models have been extended to include a description of π-ρ scattering, so that correlated π-ρ exchange may be included in the description of the nucleon-nucleon force [29].) It may be seen in these studies that, in the description of correlated two-pion exchange, the exchanged system has either a $q\bar{q}q\bar{q}$ structure or a $q\bar{q}q\bar{q}q\bar{q}$ structure. Therefore, the model of correlated two-pion exchange in Refs. [26] and [27] is quite different than the one advocated in our work.

Support for our analysis comes from the study of QCD sum rules in matter [12,18]. In that work one finds large (attractive) scalar-isoscalar and large (repulsive) vector-isovector density-dependent components in the nucleon self-energy in matter. The nucleon mass in matter is reduced significantly, the reduction being as large as 30-35 percent. That feature may be understood by noting that the nucleon mass in matter is largely dependent upon the value of the condensate $<\bar{q}q>_\rho$, where the subscript ρ denotes an evaluation of the matrix element at finite matter density.

There exists a model-independent relation that relates the value of the condensate in matter to the pion-nucleon sigma term σ_N. To first order in the density, we have

$$<\bar{q}q>_\rho = <\bar{q}q>_0 \left[1 - \frac{\sigma_N \rho}{f_\pi^2 m_\pi^2} \right] \quad , \tag{6.2}$$

with $\sigma_N = 45 \pm 8$ MeV being the currently accepted value. In the simplest analysis, the ratio of the nucleon mass in matter, $\tilde{m}_N$, to the mass in vacuum is then

$$\frac{\tilde{m}_N}{m_N} = \left[1 - \frac{\sigma_N \rho}{f_\pi^2 m_\pi^2} \right] \quad . \tag{6.3}$$

(See Ref. [19] for further discussion of these matters.)

The point we wish to stress is that the relevant order parameter is $<\bar{q}q>_\rho$, which does not involve two-pion states. (Two-pion states would be represented by order parameters of $\bar{q}q\bar{q}q$ structure.) Further, the relation between the sigma field in matter and the condensate $<\bar{q}q>_\rho$ is obtained from a bosonization scheme. One may write

$$\sigma = -\frac{G_S}{g_{\sigma qq}}\left[<\bar{q}q>_\rho - <\bar{q}q>_0\right] \quad . \tag{6.4}$$

(Note that the total sigma field is $\sigma_T = f_\pi + \sigma$, where f_π is the vacuum value.) Therefore, we see that our analysis of correlated two-pion exchange is consistent with the QCD sum-rule analysis, since, for spacelike values of t, the various amplitudes considered are dominated by exchange of the sigma, a $\bar{q}q$ excitation that is the chiral partner of the pion.

Acknowledgement

This work was supported in part by a grant from the National Science Foundation and by the PSC-CUNY Faculty Award Program.

References

[1] R. Machleidt, in Advances in Nuclear Physics, Vol. 19, eds. J.W. Negele and E. Vogt (Plenum, New York, 1989).

[2] G.E. Brown and A.D. Jackson, The Nucleon-Nucleon Interaction (North-Holland, Amsterdam, 1976).

[3] J.W. Durso, M. Saavela, G.E. Brown, and B.J. Verwest, Nucl. Phys. A278, 445 (1977).

[4] J.W. Durso, A.D. Jackson, and B.J. Verwest, Nucl. Phys. A345, 471 (1980).

[5] W. Lin and D.B. Serot, Nucl. Phys. A512, 637 (1990).

[6] J.F. Donoghue, E. Golowich, and B.R. Holstein, Dynamics of the Standard Model (Cambridge University Press, New York, 1992).

[7] Y. Nambu and G. Jona-Lasinio, Phys. Rev. 122, 345 (1961); ibid. 124, 246 (1961).

[8] We find the momentum-space bosonization scheme of V. Bernard, A.A. Osipov, and Ulf-G. Meissner, Phys. Lett. B285, 119 (1992) to be quite useful.

[9] L.S. Celenza, C.M. Shakin, Wei-Dong Sun, J. Szweda, and Xiquan Zhu, Intl. J. Mod. Phys. E2, 603 (1993). In this reference Re $C(P^2)$ should be replaced by Re $C(P^2) + \hat{J}_S(P^2)$. [See Eq. (3.16).]

[10] L.S. Celenza, C.M. Shakin, and J. Szweda, Intl. J. Mod. Phys. E2, 437 (1993).

[11] B.C. Clark, in Relativistic Dynamics and Quark-Nuclear Physics, edited by M.B. Johnson and A. Picklesimer (Wiley, New York, 1986).

[12] T.D. Cohen, R.J. Furnstahl, and D.K. Griegel, Phys. Rev. Lett. 67, 961 (1991).
T. Hatsuda, H. Høgaasen, and M. Prakash, Phys. Rev. C42, 2212 (1990).
C.M. Shakin, Phys. Rev. C50, 1129 (1994).

[13] C. Schütz, J.W. Durso, K. Holinde, and J. Speth, Phys. Rev. C49, 2871 (1994).

[14] T.P. Cheng and R. Dashen, Phys. Rev. Lett. 26, 594 (1971).

[15] L.S. Celenza, C.M. Shakin, Wei-Dong Sun J. Szweda, and Xiquan Zhu, Phys. Rev. D51 (April 1, 1995 issue).

[16] L.S. Celenza, C.M. Shakin, Wei-Dong Sun, J. Szweda, and Xiquan Zhu, Brooklyn College Report: BCCNT 94/601/232R3 (1994). To be published in Ann. Phys. (N.Y.) in July 1995.

[17] C.M. Shakin, Wei-Dong Sun, and J. Szweda, Brooklyn College Report: BCCNT 94/602/233R3 (1994). To be published in Ann. Phys. (N.Y.) in July 1995.

[18] R.J. Furnstahl, D.K. Griegel, and T. Cohen, Phys. Rev. C46, 1507 (1992);
X. Jin, T.D. Cohen, R.J. Furnstahl, and D.K. Griegel, Phys. Rev. C47, 2882 (1993).
X. Jin, M. Nielsen, T.D. Cohen, R.J. Furnstahl, and D.K. Griegel, Phys. Rev. C49, 464 (1994);
X. Jin and R.J. Furnstahl, Phys. Rev. C49, 1190 (1994);
X. Jin and M. Nielsen, Phys. Rev. C51, 347 (1995).

[19] L.S. Celenza, A. Pantziris, C.M. Shakin, and Wei-Dong Sun, Phys. Rev. C45, 2015 (1992); L.S. Celenza, A. Pantziris, C.M. Shakin, and Wei-Dong Sun, Phys. Rev. C46, 57 (1992); L.S. Celenza, C.M. Shakin, Wei-Dong Sun, and Xiquan Zhu, Phys. Rev. C48, 159 (1993).

[20] L.S. Celenza, A. Pantziris, and C.M. Shakin, Phys. Rev. C46, 2213 (1992).
In this work we calculated the two-nucleon-irreducible matrix elements of the interaction for insertion in a Bethe-Salpeter equation, for example. Therefore, we did not attempt to demonstrate the equivalence of pseudoscalar and pseudovector coupling schemes.

[21] C.A. da Rocha and M.R. Robilotta, Phys. Rev. C49, 1818 (1994).

[22] C. Ordonez, L. Ray, and U. van Kolck, Phys. Rev. Lett. 72, 1982 (1994).

[23] M. Birse, Phys. Rev. C49, 2212 (1994).

[24] K. Holinde, preprint KFA-IKP(TH) – 1994-41. Invited talk presented at the Conference on Physics with GeV-Particle Beams, Jülich, Germany (Aug. 22-25, 1994).

[25] G. Höhler, F. Kaiser, R. Koch, and E. Pietarinen, Handbook of Pion-Nucleon Scattering, Physics Data 12-1, Fachinformationszentrum, Karlsruhe, 1979.

[26] H.-C. Kim, J.W. Durso, and K. Holinde, Phys. Rev. C49, 2355 (1994).

[27] C. Schütz, K. Holinde, J. Speth, B.C. Pearce, and J.W. Durso, Phys. Rev. C51, 1374 (1995).

[28] D. Lohse, J.W. Durso, K. Holinde, and J. Speth, Nucl. Phys. A516, 513 (1990).

[29] G. Janssen, K. Holinde, and J. Speth, Phys. Rev. C49, 2763 (1994).

Figure Captions

Fig. 1. (a) The T matrix for $\pi - N$ scattering in the s channel ($\pi N \to \pi N$) and for pion production in the t channel ($N\bar{N} \to 2\pi$) is shown.

(b) A t-channel exchange process defined for $t < 0$ and $s > (m_\pi + m_N)^2$ is shown. (The coupling of the sigma meson to the nucleon is taken as $G_{\sigma NN} \sim 3g_{\sigma qq} \sim 9$ [1]. (It is possible to use a smaller value of $G_{\sigma NN}$ if other sources of scalar-isoscalar attraction are treated explicitly.)

Fig. 2. The $N + \bar{N} \to \pi + \pi$ helicity amplitude, $\mathrm{Im}\, f_+^0(t)$, is shown. The values of this amplitude were obtained in Ref. [25].

Fig. 3. (a) General form of coupled equations for the T matrices t_{qq}, $t_{q\pi}$ and $t_{\pi\pi}$. (See Ref. [16].)

(b) The form of the kernals, $k_{q\pi}$ and $k_{\pi q}$, used in this work is shown.

(c) The interaction k_{qq} is shown to be composed of the Born term of the NJL model (black dot) and a confining field V^C.

Fig. 4. (a) The basic quark-loop integral of the NJL model is shown. In the notation of this work we have $P^2 = t$. [See Eq. (3.1).]

(b) The function $\hat{J}_S(P^2)$ is defined by introducing a vertex (cross-hatched area) for the confining interaction V^C. See Ref. [15] for a detailed discussion of the construction of such vertex functions.

(c) The function $K_S(P^2)$ is defined by the diagram shown. (See Ref. [9].)

(d) The function $\hat{K}_S(P^2)$ is defined by including a vertex function for the confining interaction (cross-hatched region). (See Ref. [15].)

Fig. 5. The function Re $\hat{M}(P^2)$ is shown as a solid line. The dashed line is Im $\hat{M}(P^2)$. Note that $\hat{M}(P^2) = -G_S^2 \hat{K}_S(P^2)$. (This figure is taken from Ref. [9].)

Fig. 6. (a) Some box-diagrams and s-channel meson exchange interactions neglected in our solution of the coupled quark-hadron equations are shown.

(b) A diagrammatic element that appears in model C but is absent in model B. [See Eqs. (3.2) and (3.3).]

(c) Some of the diagrams summed to obtain the $q\bar{q}$ T matrix of model C. [See Eq. (3.2).] The black dots denote the basic interaction of the NJL model.

Fig. 7. (a) The T matrix $t_{q\pi}$ for the process $q + \bar{q} \to \pi + \pi$ is shown.

(b) The T matrix for the process $q + \bar{q} \to \pi + \pi$ in the t channel with $J = 0$ and $T = 0$ is shown in a schematic fashion. By expanding the denominator, $D^B(t)$, the various diagrams shown are generated. [See Eqs. (3.5) and (3.9).]

(c) Basic diagrammatic element that connects the $q\bar{q}$ states to the two-pion continuum. [See (b) above.]

Fig. 8. (a) The diagrammatic series of Fig. 7(b) is shown for $t < 0$, where $\hat{K}_S(t)$ may be neglected.

(b) In the pseudophysical region of the t channel ($t < 0$) the diagrammatic series shown in (a) can be replaced by diagram shown. Here the coupling of the sigma meson to the quark is $g_{\sigma qq}$. In this work we use $g_{\sigma qq} = 3.05$.

Fig. 9. The imaginary part of the correlator $C(t)$ is shown as a dashed line. The calculation is made using model B and is described in Ref. [9]. The solid line represents Re $C(t) + \hat{J}_S(t)$ and is obtained via a dispersion relation. The dotted line denotes a sigma-dominance approximation with $C(t) + \hat{J}_S(t) = a^2/(t^2 - m_\sigma^2)$. Here $a = 0.0511$ GeV^4 and $m_\sigma = 0.540$ GeV. The dotted line provides a good fit to the solid line over a broad range of $t < 0$.

Fig. 10. The dashed line and the solid line for $t < 0$ denote the values of $\hat{J}_S(t)$ calculated in a Euclidean momentum space with $\Lambda = 1.0$ GeV. The solid line for $t > 0$ represents the result of a calculation of $\hat{J}_S(t)$. A three-dimensional cutoff of $\Lambda_3 = 0.702$ GeV is used for all the momentum vectors in the integral. Here we use $m_q = 262$ MeV and the model of confinement described in Ref. [15]. Note that the inclusion of the confinement vertex functions hardly affects the result for $t < 0$.

Fig. 11. The figure exhibits the value of $F(t)/12$ for both spacelike and timelike values of t. Here $12 = 2n_c n_f$ is a statistical factor. For $t < 4m_q^2$ the solid curve represents a calculation made in Euclidean space. For $t > 4m_q^2$, the solid line denotes the result of a Minkowski-space

calculation including a vertex function of the confining field. We use m_q = 262 MeV, $g_{\pi qq}$ = 3.05 and the same cutoffs as given in the caption of Fig. 10. Note that from Eq. (3.12), $F(0) = 2g_{\sigma\pi\pi}/g_{\sigma qq}$. In our calculation, that relation is well satisfied, if we put m_σ = 542 MeV in Eq. (3.13) and use $g = g_{\sigma qq}$ = 3.05. (We see that $f_\pi = m_q/g$ = 0.086 GeV and $F(0)/12$ = 0.093 GeV.)

Fig. 12. (a) A sigma-dominance approximation for the quark-antiquark interaction, valid for $t < 0$, is shown. [See Eq. (3.8).]

(b) A sigma-dominance approximation for the amplitude $q + \bar{q} \to \pi + \pi$. (See Eq. (3.11). Values of $F(t)$ are shown in Fig. 11.)

(c) A sigma-dominance approximation for the correlator $C(t) + \hat{J}_S(t)$ is shown. This approximation is valid for $t < 0$. (See the dotted line in Fig. 9. For $t < 0$ the dotted line and the solid line representing Re $C(t) + \hat{J}_S(t)$ are indistinguishable.)

Fig. 13. The figure exhibits Re $t_{qq}(t)$ [solid line] and Im $t_{qq}(t)$ [dashed line] obtained using model B where $t_{qq}(t)$ is given by Eq. (3.3). The dotted line represents $g^2/(t - m_\sigma^2)$ with g = 3.05 and m_σ = 0.542 GeV. The values for $\hat{J}_S(t)$ to be inserted in Eq. (3.3) are taken from Fig. 10. (We put $\hat{J}_S(t) = J_S(t)$ for $t < 0$.) Note that if we were to neglect $\hat{K}_S(t)$, we would have $t_{qq}(0) \simeq -23$ GeV^2. The dotted curve provides a good fit to the solid curve for -0.2 GeV$^2 < t \leq 0$. This is the range of

momentum transfer that is particularly important for nuclear structure physics and for nucleon-nucleon scattering.

Fig. 14. The values of Re $t_{q\pi}(t)$ [solid line] and Im $t_{q\pi}(t)$ [dashed line] are shown. Values of $t_{qq}(t)$ and $F(t)$ needed to form $t_{qq}(t)$ are shown in Figs. 11 and 13, respectively. [See Eq. (3.9).]

Fig. 15. (a) On the left-hand side we show a generic diagram used to represent correlated two-pion exchange [2]. The first diagram on the right-hand side denotes the quark-quark interaction of the NJL model. The last diagram introduces the scalar-isoscalar correlation function. That correlation function has a cut for $t > 4m_\pi^2$ and describes correlated two-pion exchange.

(b) The correlation function of (b) may be given in terms of $\hat{J}_S(t)$ and a T matrix of general form. In this work we limit our considerations to the forms $t_{qq}^C(t)$ and $t_{qq}^B(t)$ given in Eqs. (3.2) and (3.3). (These are T matrices expressible in terms of $\hat{J}_S(t)$ and $\hat{K}_S(t)$ only.)

(c) For $t < 0$, the diagrams of (b) may be replaced by the diagram shown. That may be seen by noting that $t_{qq}(t) = -G_S/[1 - G_S\hat{J}_S(t)]$ for $t < 0$, where $\hat{K}_s(t)$ may be neglected. The coupling of the sigma to the nucleon is approximately $G_{\sigma NN} \simeq 3g_{\sigma qq} \simeq 9$.

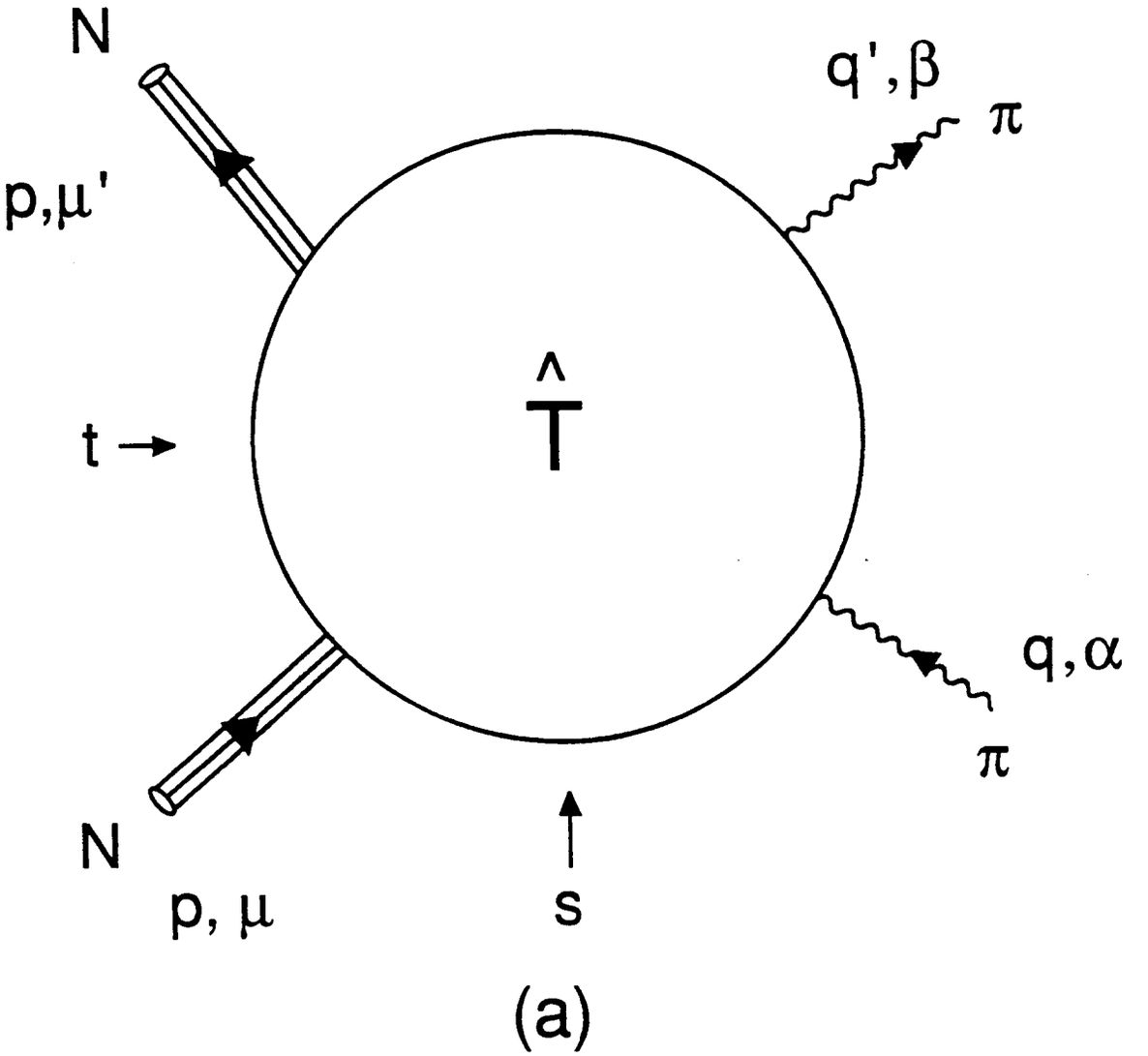

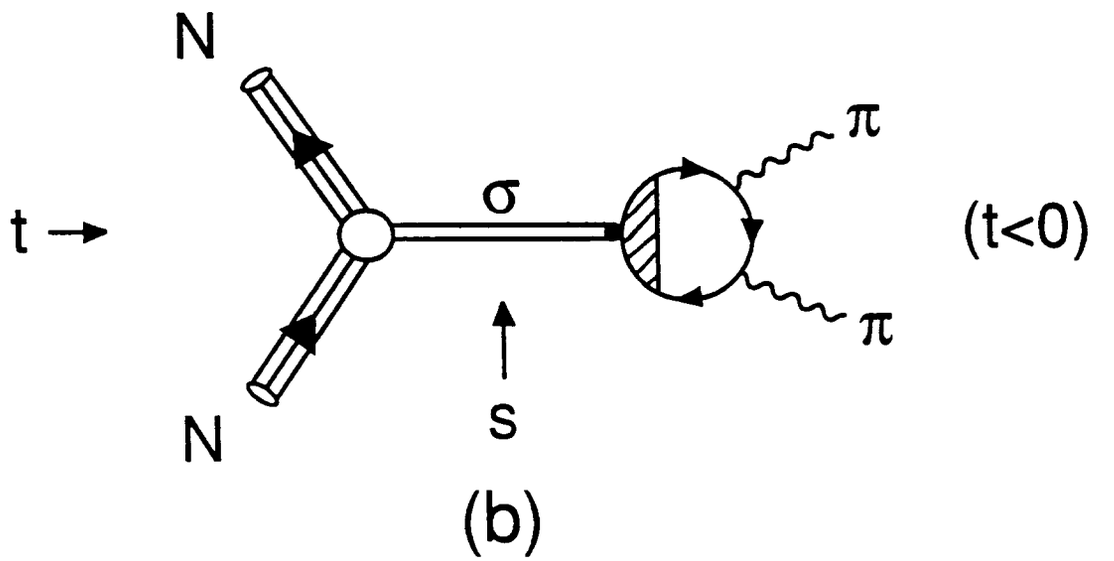

FIG. 1

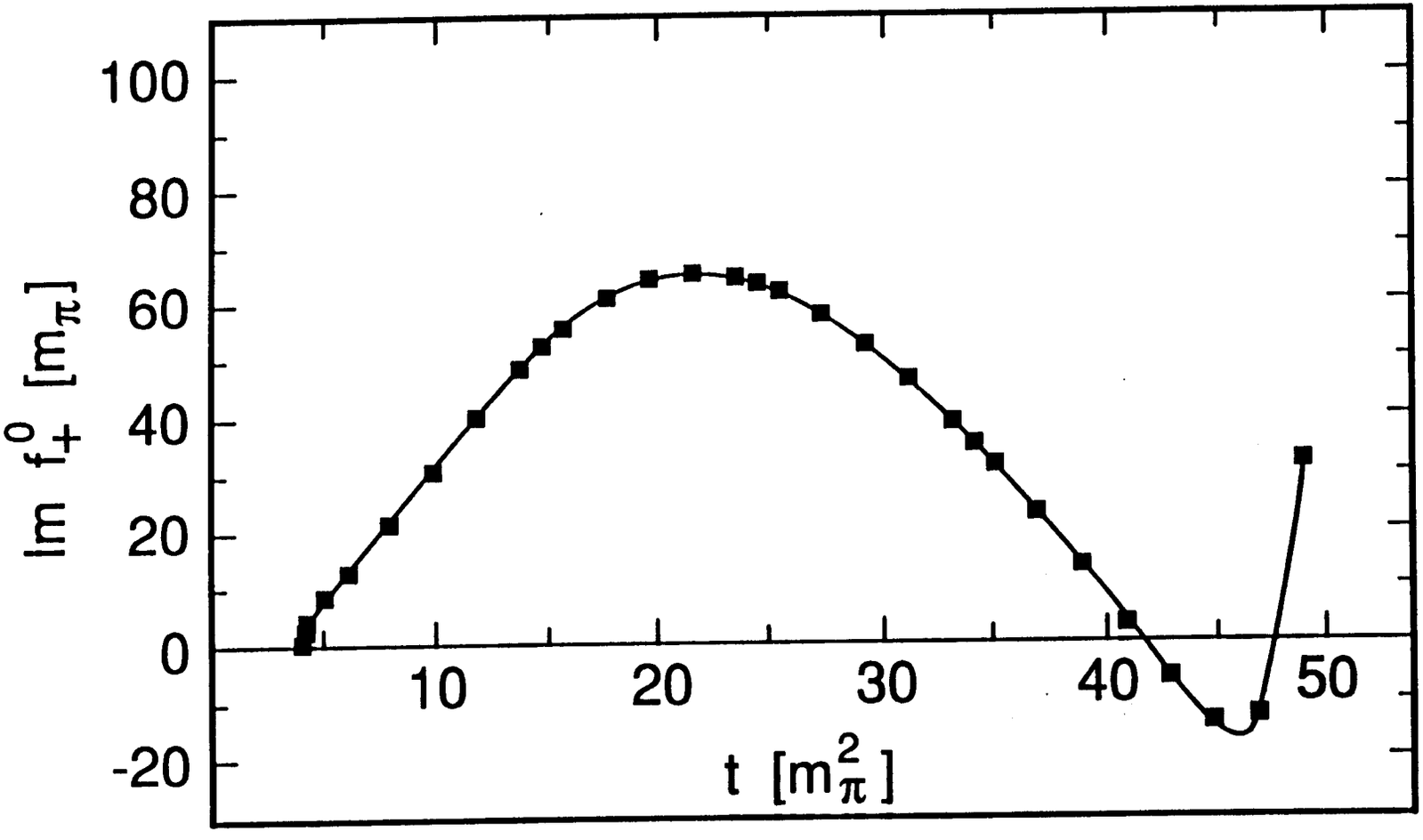

FIG. 2

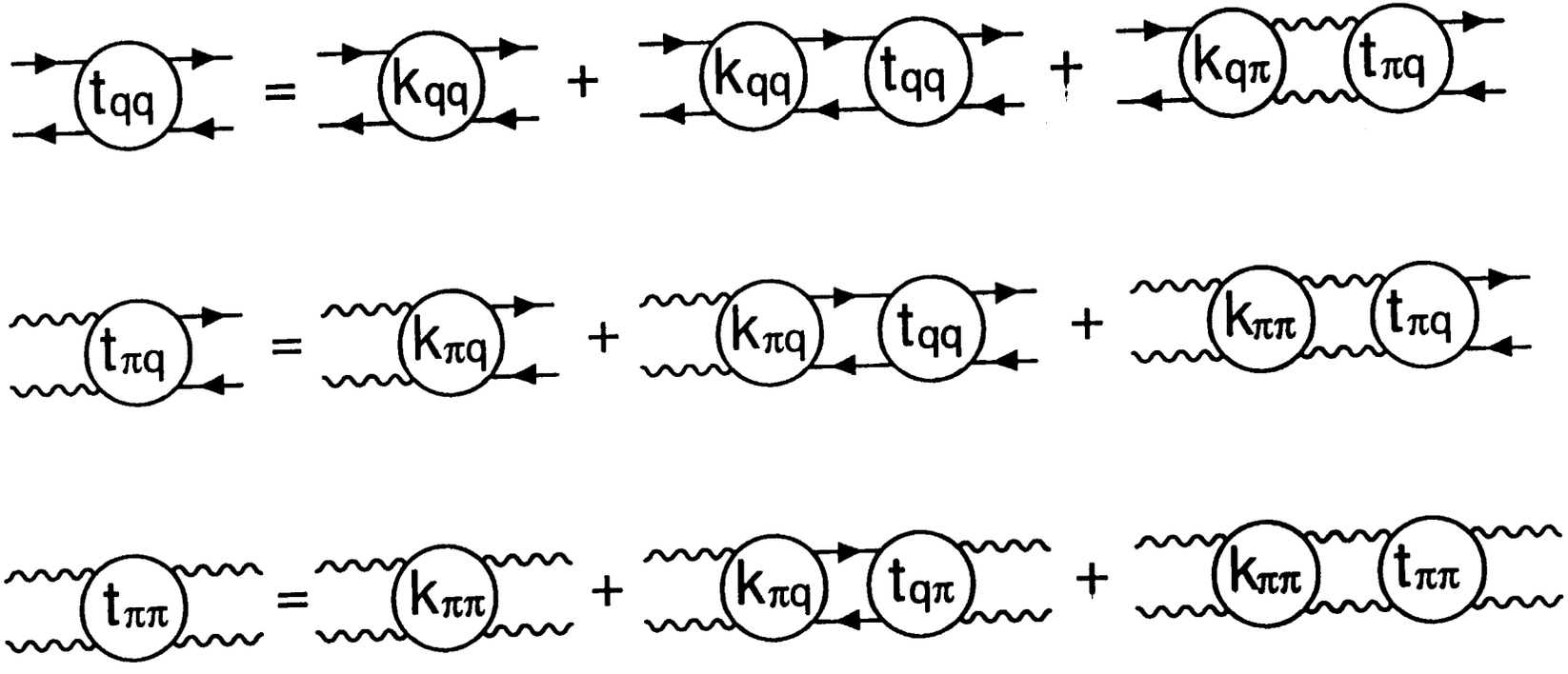
t_{qq} = k_{qq} + k_{qq} t_{qq} + $k_{q\pi}$ $t_{\pi q}$
$t_{\pi q}$ = $k_{\pi q}$ + $k_{\pi q}$ t_{qq} + $k_{\pi\pi}$ $t_{\pi q}$
$t_{\pi\pi}$ = $k_{\pi\pi}$ + $k_{\pi q}$ $t_{q\pi}$ + $k_{\pi\pi}$ $t_{\pi\pi}$

(a)

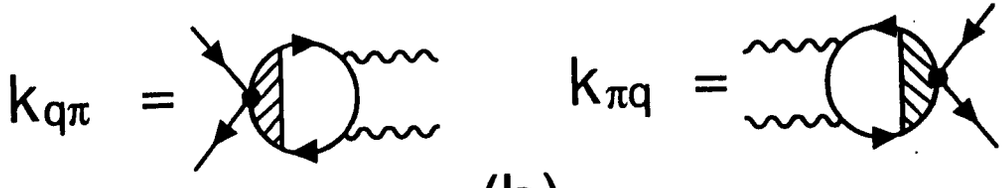
$k_{q\pi}$ =
$k_{\pi q}$ =

(b)

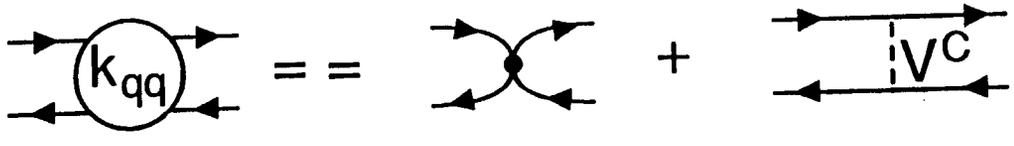
k_{qq} = =
+
V^C

(c)

FIG. 3

$-iJ_S(P^2) =$

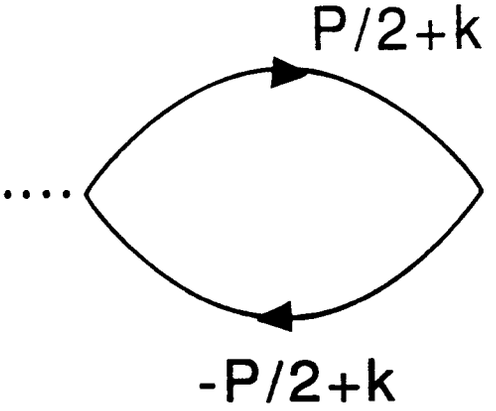

(a)

$-i\hat{J}_S(P^2) =$

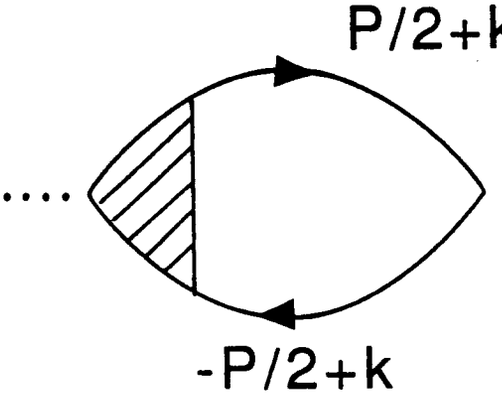

(b)

$-iK_S(P^2) =$

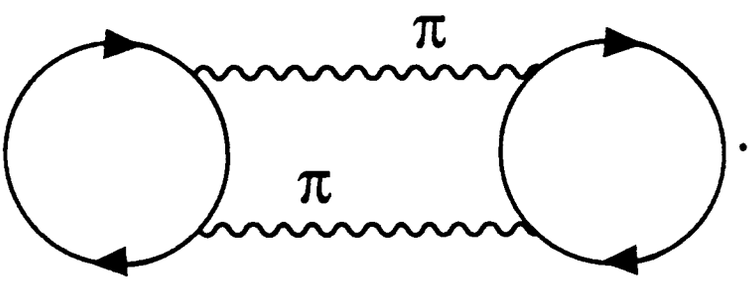

$-i\hat{K}_S(P^2) =$

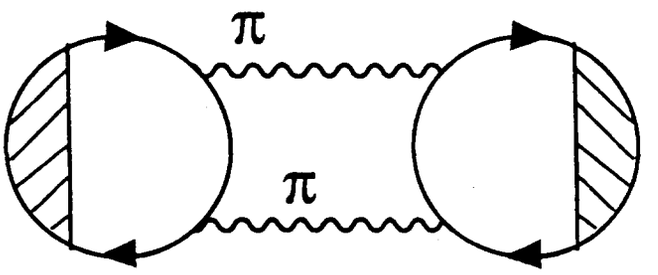

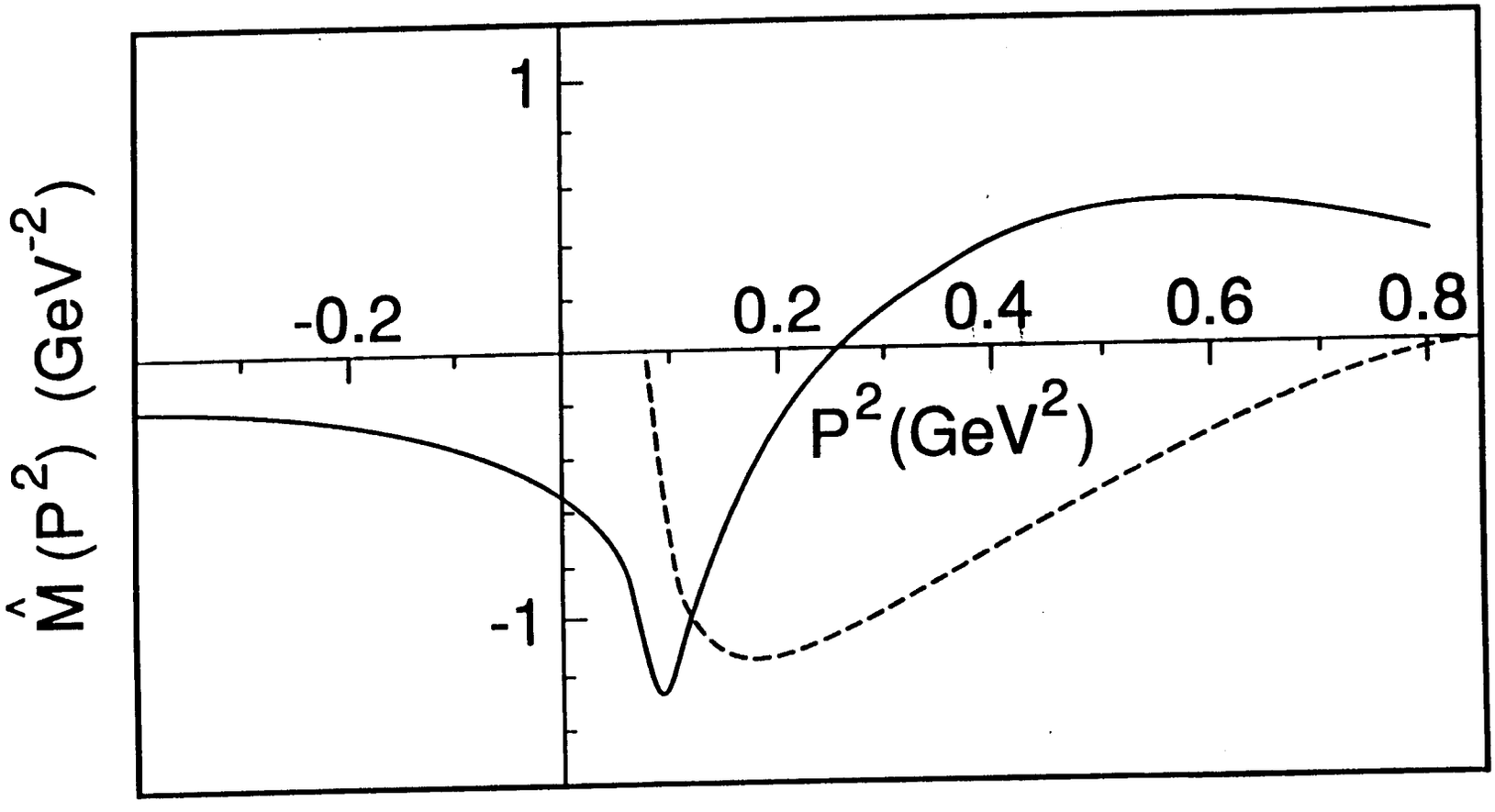

FIG. 5

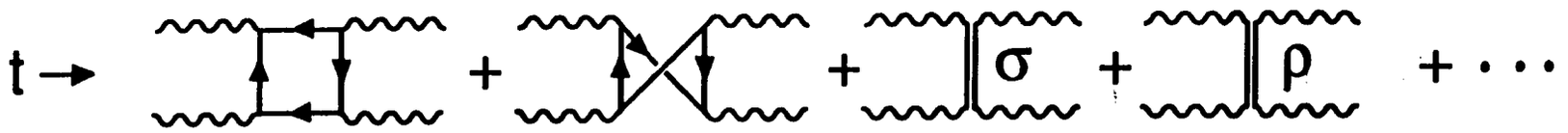

(a)

(b)

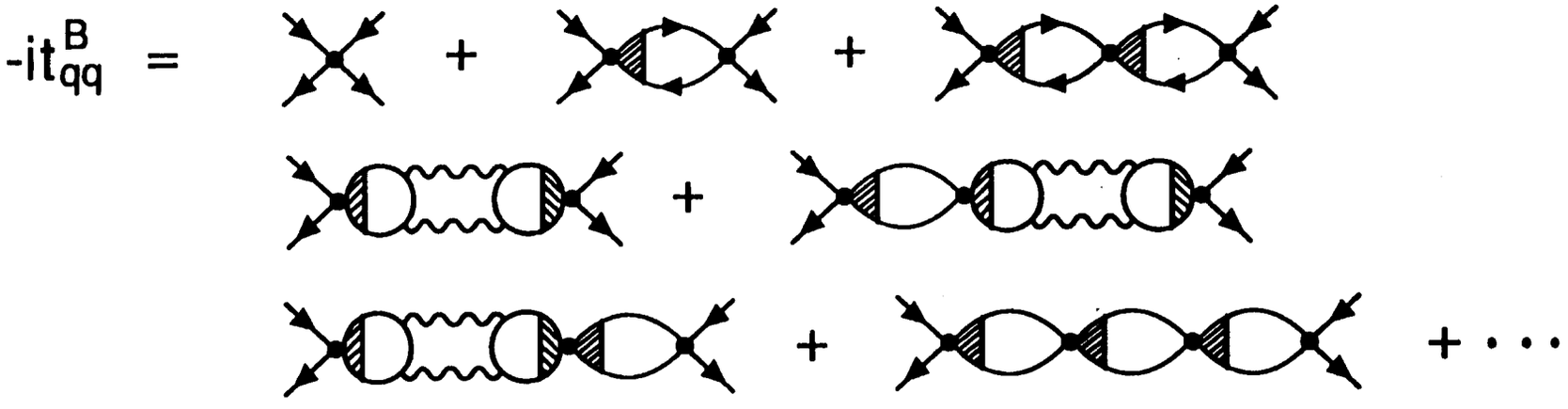

(c)

FIG. 6

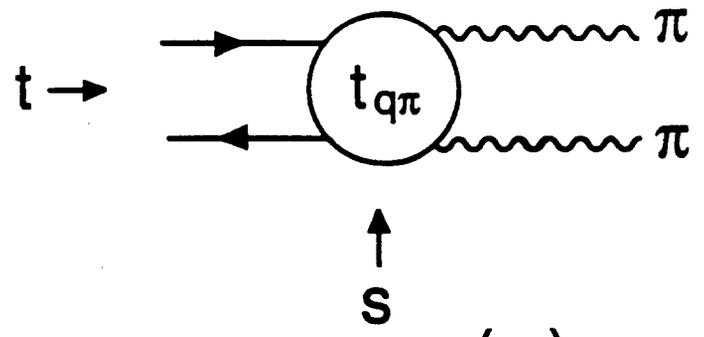

(a)

$$-it^{B}_{q\pi}(t) = \frac{1}{D^{B}(t)}$$

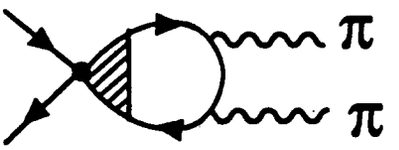

$$=$$

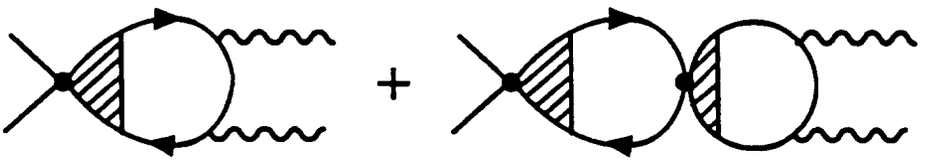

$$+$$

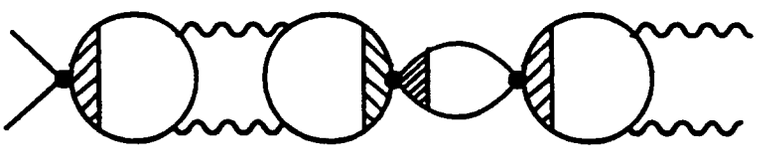

$$+ \quad \cdots$$

(b)

$$-iF(t) = \cdots$$

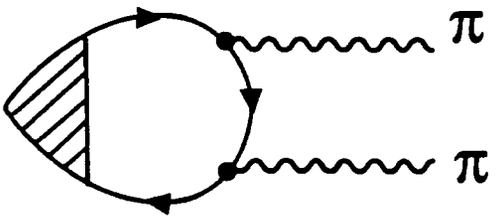

(c)

FIG 7

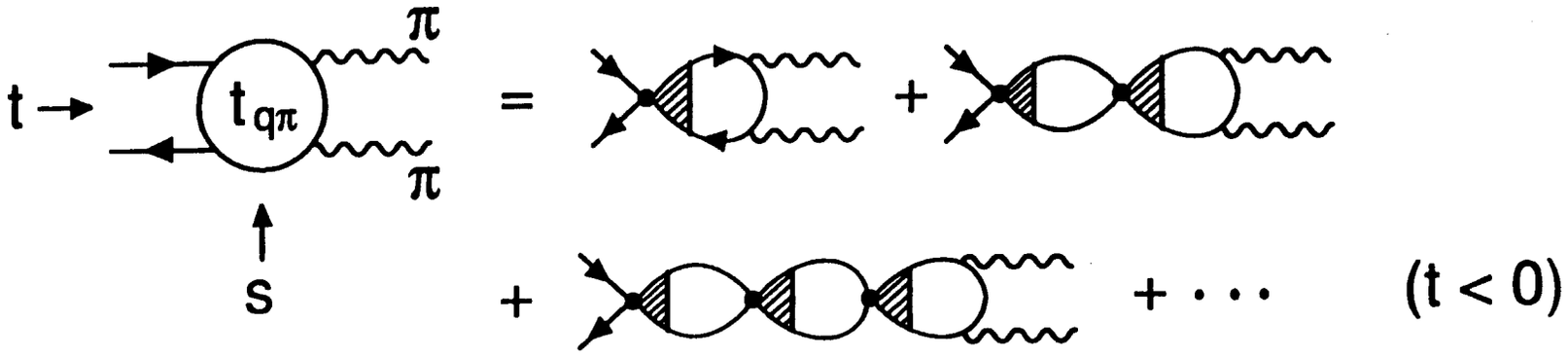

(a)

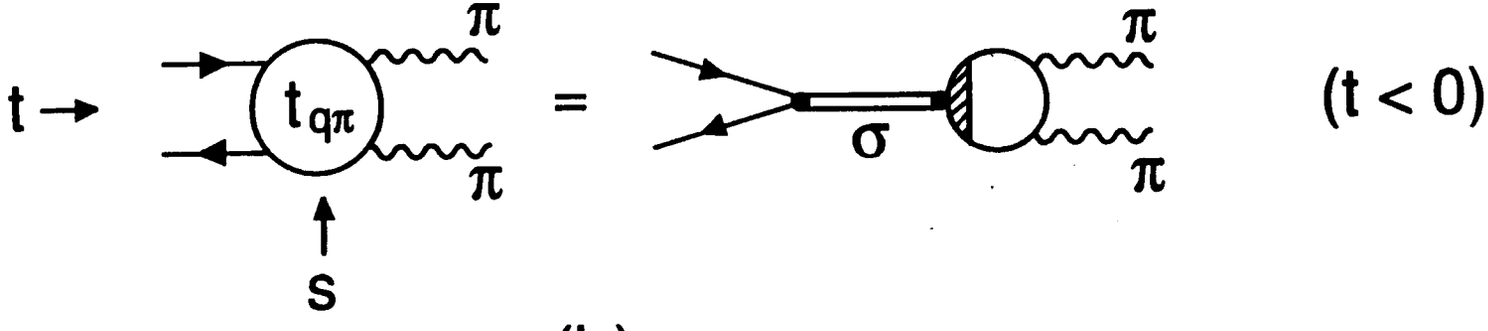

(b)

FIG. 8

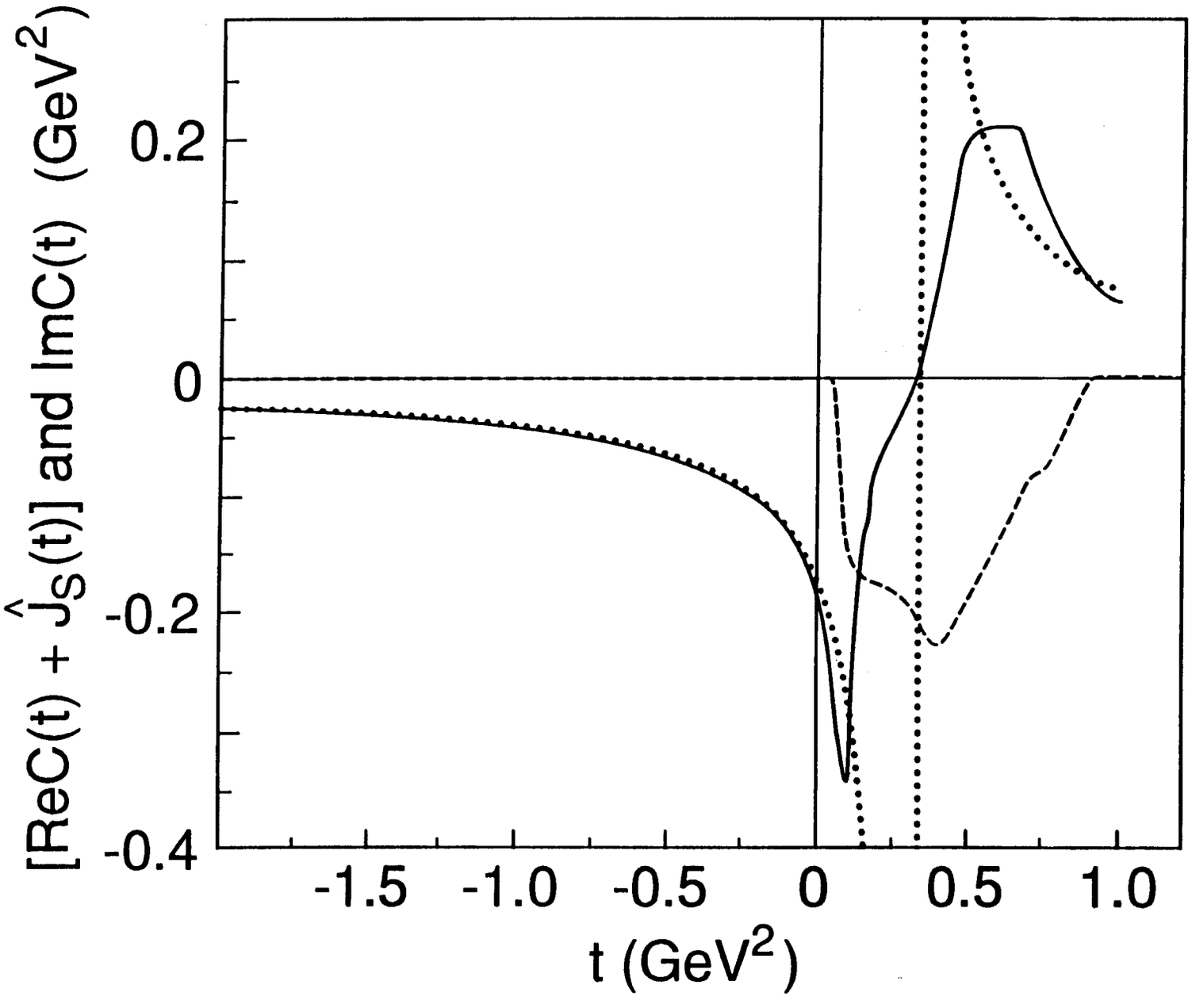

FIG. 9

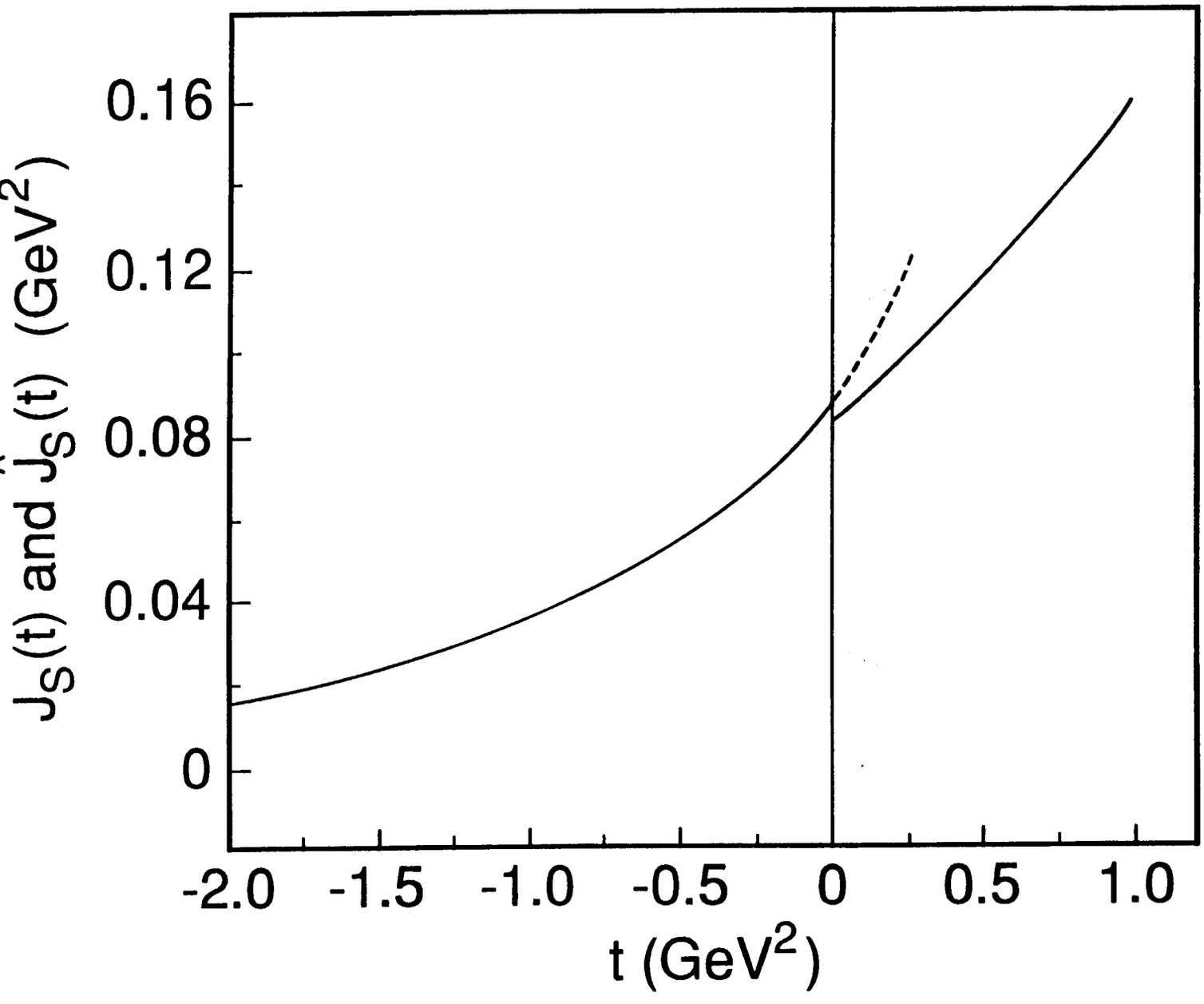

FIG. 10

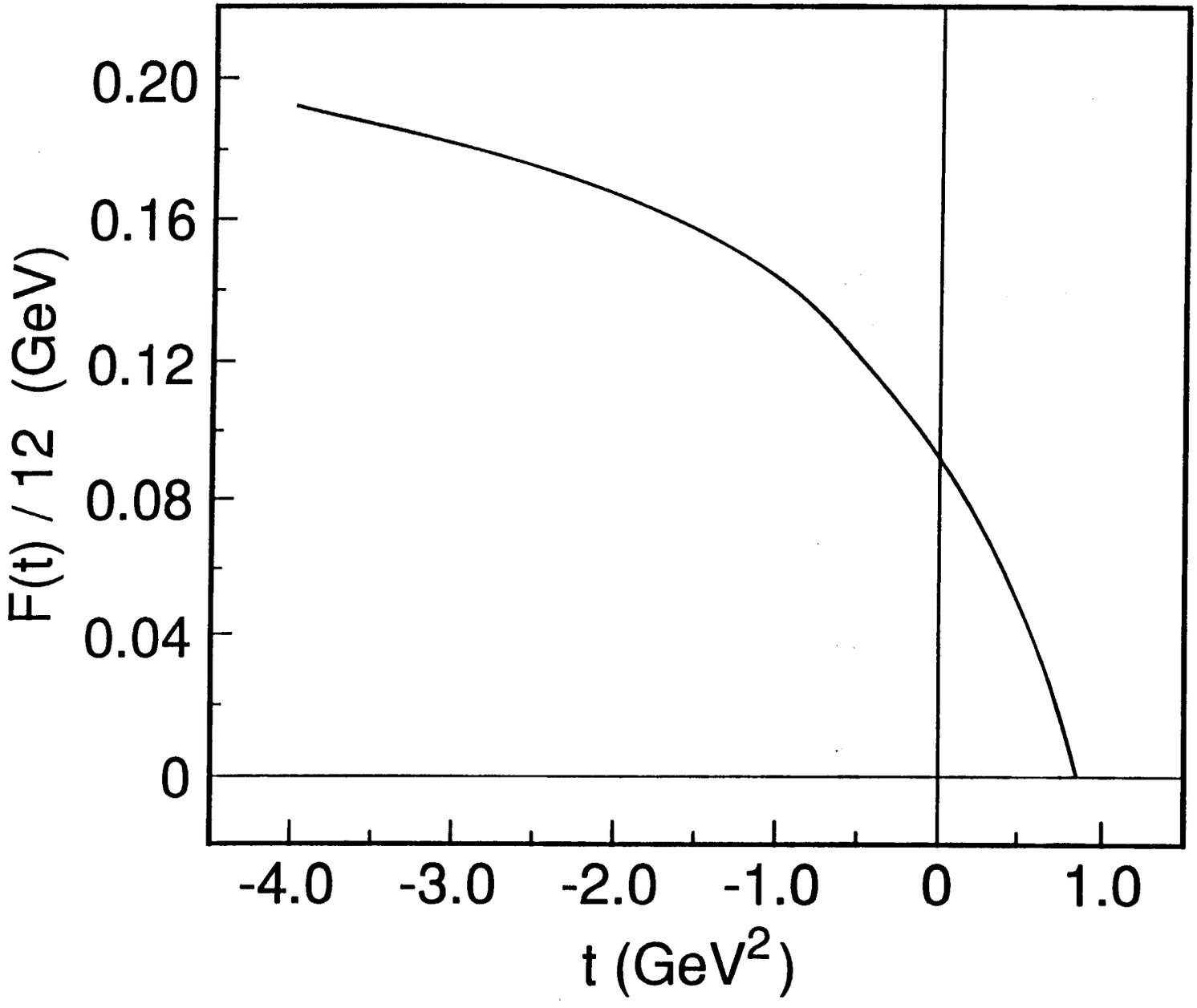

FIG. 11

$-it_{qq}(t) \sim$

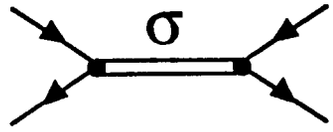

(a)

$-it_{q\pi}(t) \sim$

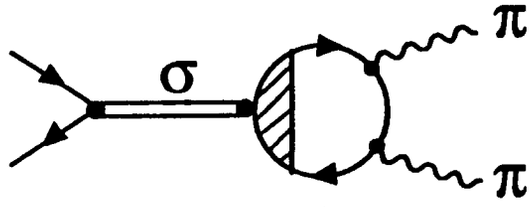

(b)

$iC(t) + i\hat{J}_S(t) \sim$

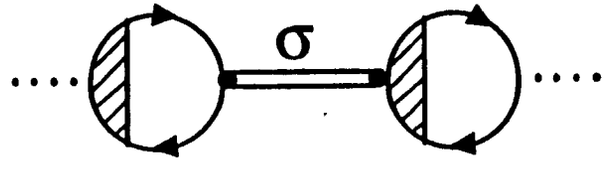

(c)

FIG. 12

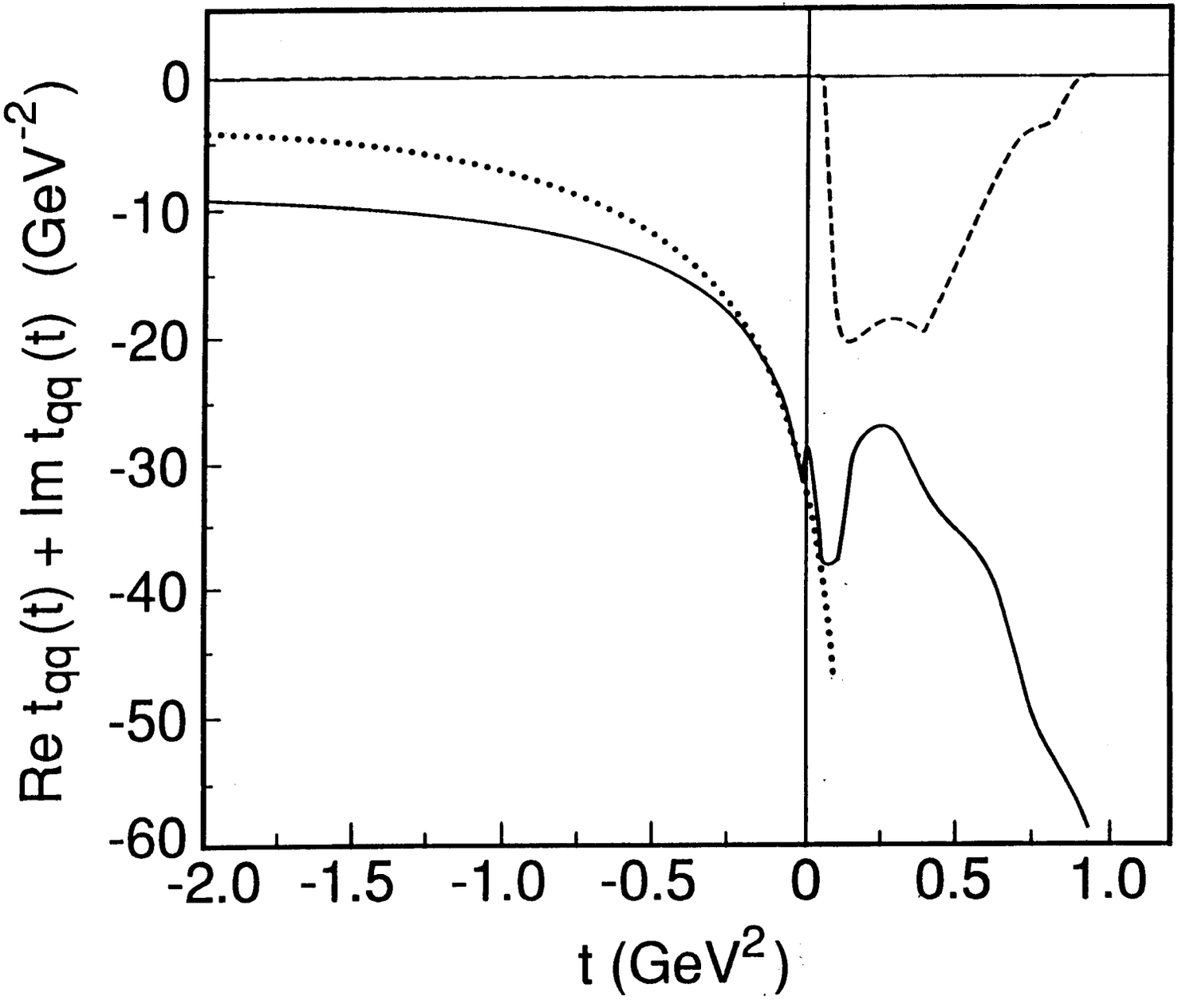

FIG. 13

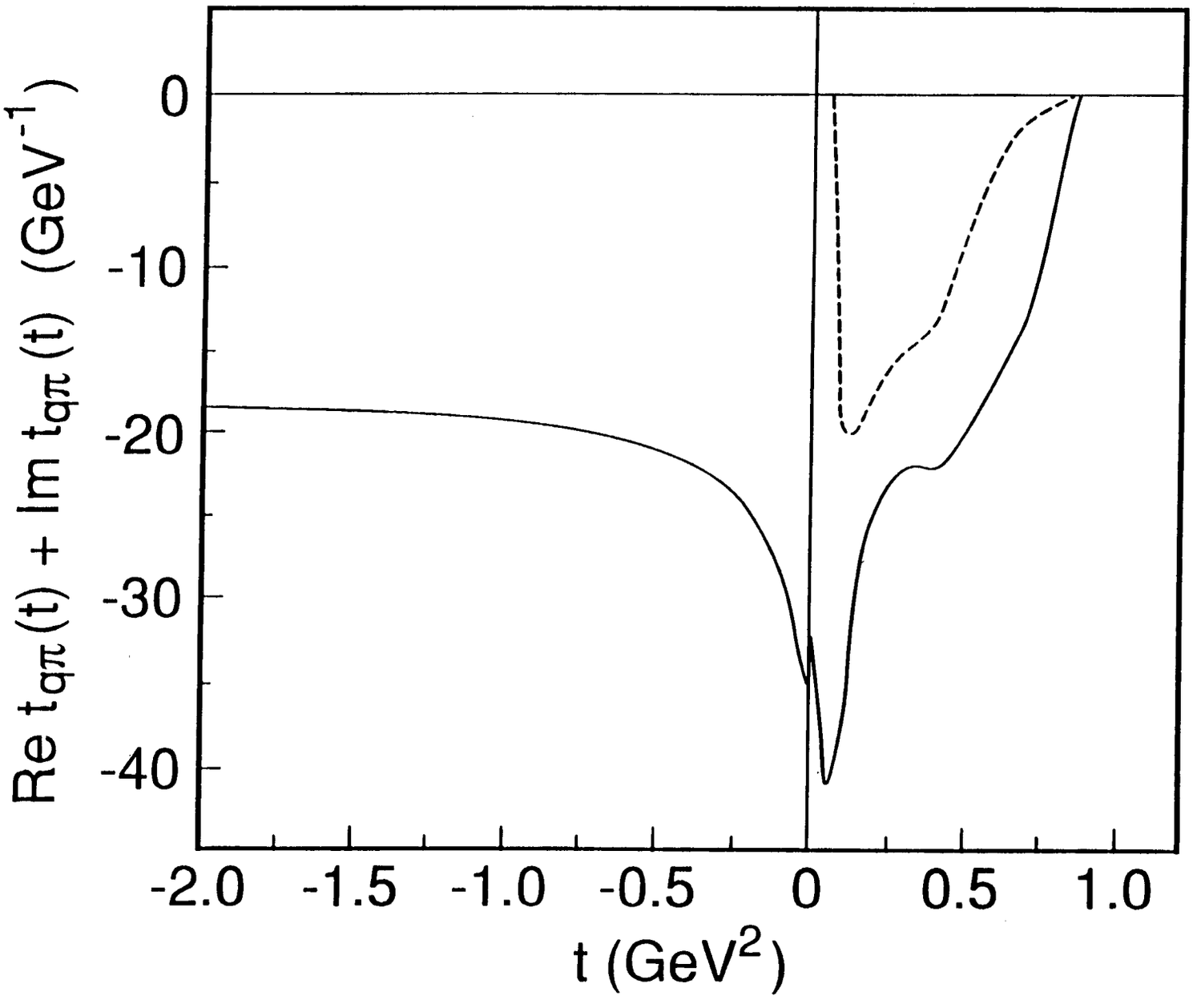

FIG. 14

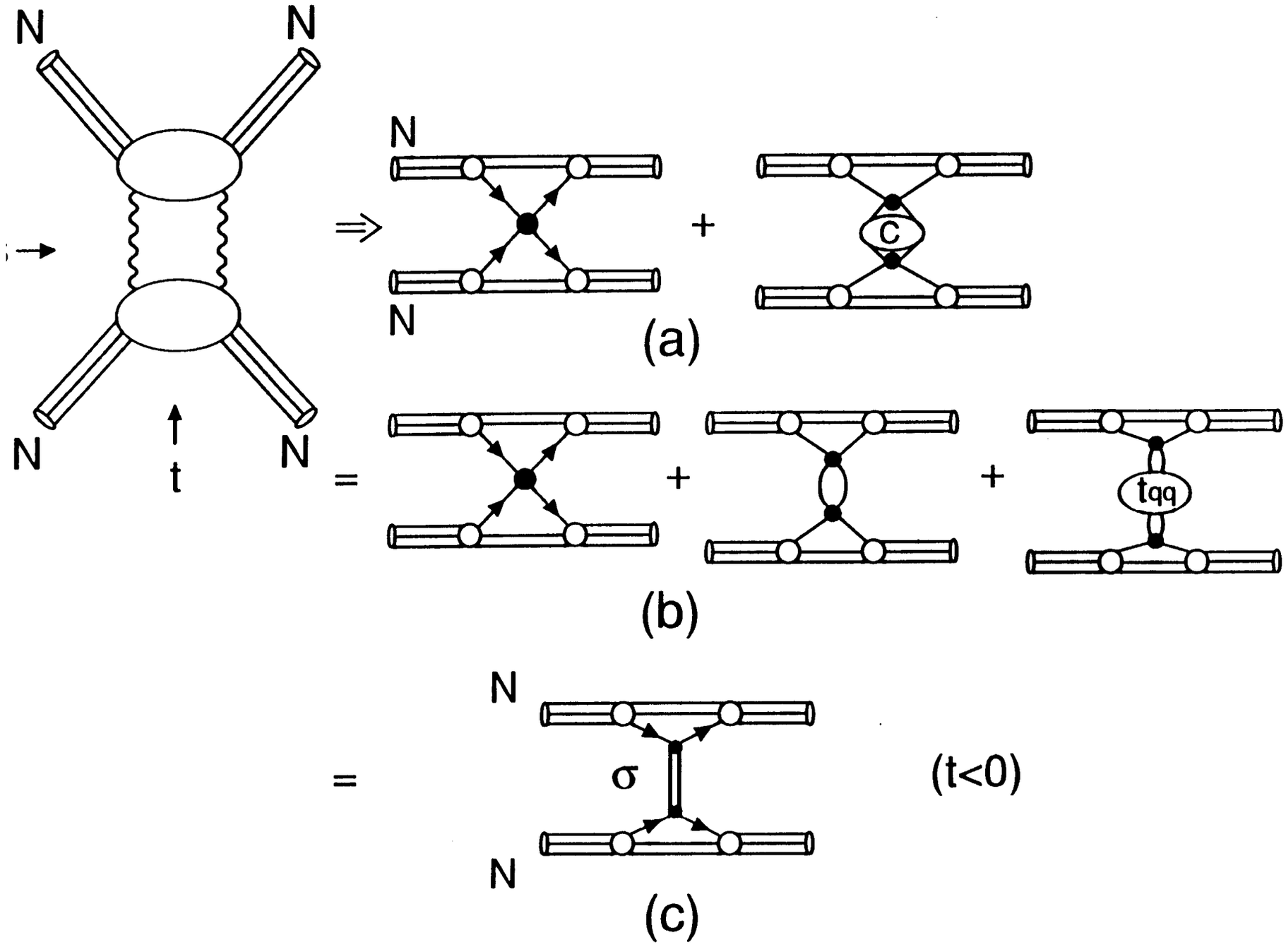

FIG. 15